34th Annual International Conference of the IEEE EMBS
San Diego, California USA, 28 August - 1 September, 2012

Compressed Sensing for Integral Pulse Frequency Modulation (IPFM)-based Heart Rate Variability Spectral Estimation

Szi-Wen Chen, *Member, IEEE*, and Shih-Chieh Chao

Abstract— **In this paper, a Compressed Sensing (CS) based spectral analysis of Heart Rate Variability (HRV) using the Integral Pulse Frequency Modulation (IPFM) model is introduced. Previous research in literature indicated that the IPFM model is considered as a functional description of the cardiac pacemaker and thus is very useful in modeling the mechanism by which the Autonomic Nervous System (ANS) modulates the Heart Rate (HR). On the other hand, in recent years CS has attracted great attention over many aspects of signal processing applications. According to the IPFM model, we here present a CS-based algorithm for deriving the amplitude spectrum of the modulating signal for HRV assessments. In fact, the application of the CS method into HRV spectral estimation is novel and unprecedented in HRV analysis. Numerical experimental results demonstrated that the proposed approach can robustly yield accurate HRV spectral estimates, even under the situation of a degree of incompleteness in the interbeat interval or RR data caused by ectopic or missing beats.**

I. INTRODUCTION

Previous studies in literature have reported that Heart Rate Variability (HRV) analysis provides an insight into the mechanism of Autonomic Nervous System (ANS) activity [1]. In clinical situation, the analysis results of HRV may be also used for evaluating the condition of the patient's heart. In general, there are a number of different methods developed based on time and frequency domain for quantifying the variability in HR, including the calculation of the standard deviation of interbeat intervals and/or the power spectral analysis of the HR fluctuations. In these applications, the beat-to-beat variations are quantitatively captured simply by processing the interbeat interval sequence which is directly, noninvasively derived from the Electrocardiogram (ECG) data. On the other hand, since the HRV reflects the information of the underlying ANS control activities, in contrast to the direct beat-to-beat interval analysis we may also obtain the information related to ANS control that is not directly measurable simply using a modeling analysis. In this aspect, a model referred to as the Integral Pulse Frequency Modulation (IPFM) has been extensively discussed in previous research in literature [2]-[5]. Although the IPFM model has been well applied for the generation and validation of HRV spectra, theoretical derivation of a robust spectral analysis of IPFM-based HRV has not been completely and well developed.

S.-W. Chen is with the Dept. of Electronic Engineering, Chang Gung University, Tao-Yuan, Taiwan (e-mail: chensw@mail.cgu.edu.tw).

S.-C. Chao is with the Dept. of Electronic Engineering, Chang Gung University, Tao-Yuan, Taiwan (e-mail: vrchao@gmail.com).

In recent years, Compressed Sensing or Compressive Sensing (CS) has been considered one of the 'booming' topics in signal processing [6, 7]. It is a new data acquisition scheme that allows one to perfectly reconstruct a sparse or a compressible signal. In biomedical signal/image processing, CS has been applied to a variety of topics [8, 9], but there still remains a lack in its applications into HRV or the related analysis. The contribution of this work is that we successfully apply CS framework to an IPFM model-based HRV spectral analysis and break the bottleneck caused by the loss or incorrectness of RR intervals due to the ectopic beats or the misclassification of QRS complexes. Numerical experimental results produced in our study showed that the proposed method can achieve accurate HRV spectral estimation with a degree of robustness.

II. MATERIALS AND METHODS

A. A Model Used for the Generation of HR signals –Integral Pulse Frequency Modulation (IPFM) Model

IPFM model has been widely used to generate pulses from modulating signals. It provides a functional description of the mechanism by which the ANS modulates HR [3]. Suppose there are L of RR intervals, denoted as $RR_i = t_i - t_{i-1}$, where t_i is the occurrence time of the ith interval, $i = 1, \ldots, L$ and $t_0 = 0$. IPFM model suggests a linear relation among t_i, modulating signal $m(t)$ and an IPFM threshold TR:

$$\int_0^{t_i} \left[1 + m(t)\right] dt = iTR\,. \tag{1}$$

Inspired by the discrete Fourier transform (DFT), we assume

$$m(t) = \sum_{k=1}^{K} m_k(t), \tag{2}$$

and

$$m_k(t) = a_k \cos(\omega_k t) + b_k \sin(\omega_k t), \tag{3}$$

where $\omega_k = 2\pi k/T$, T is the period of $m(t)$ while a_k and b_k are real coefficients of cosine wave and sine wave at frequency ω_k, respectively. As a result, (1) becomes

$$\sum_{k=1}^{K}\left[\frac{a_k}{k}\sin(\omega_k t_i) + \frac{b_k}{k}\left(1-\cos(\omega_k t_i)\right)\right] = \frac{2\pi}{T}\left(iTR - t_i\right) \tag{4}$$

In the context of DFT, the period of $m(t)$ is equal to the available length of $m(t)$, *i.e.*, $T = t_L$. Thus, when $i = L$ we can compute

$$TR = \frac{t_L}{L} = \frac{1}{L}\sum_{i=1}^{L} RR_i \cdot \quad (5)$$

Therefore, t_i, T and TR can be easily computed, and there are still $L-1$ equations in (4) left, which can be compactly written into the matrix form: $y=Ax$, where

$$y = \frac{2\pi}{T}\begin{bmatrix} 1\cdot TR - t_1 \\ \vdots \\ (L-1)\cdot TR - t_{L-1} \end{bmatrix}, \quad (6)$$

$$A = \begin{bmatrix} \sin(\omega_1 t_1) & 1-\cos(\omega_1 t_1) & \cdots & \sin(\omega_K t_1) & 1-\cos(\omega_K t_1) \\ \vdots & \vdots & \vdots & \vdots & \vdots \\ \sin(\omega_1 t_{L-1}) & 1-\cos(\omega_1 t_{L-1}) & \cdots & \sin(\omega_K t_{L-1}) & 1-\cos(\omega_K t_{L-1}) \end{bmatrix}, \quad (7)$$

and

$$x = \left[{}^{a_1}\!/_1,\ {}^{b_1}\!/_1,\ \ldots,\ {}^{a_K}\!/_K,\ {}^{b_K}\!/_K \right]^T. \quad (8)$$

According to the dimension of A, the linear system can be classified as overdetermined, squared and underdetermined, *i.e.*,

$$y = Ax \quad \text{is} \quad \begin{cases} \text{overdetermined} \\ \text{squared} \\ \text{underdetermined} \end{cases}, \quad \text{if} \quad \begin{cases} K < (L-1)/2 \\ K = (L-1)/2 \\ K > (L-1)/2 \end{cases}. \quad (9)$$

Obviously, IPFM-based HRV spectra can be estimated by solving the linear system as indicated in (9). Previous studies in literature [4, 5] have developed methods for estimating IPFM-based HRV spectra in overdetermined and squared cases. In this study, we showed that IPFM-based HRV spectra can be also estimated in underdetermined case by taking advantage of compressed sensing, of which backgrounds and methodology are presented in the next section.

B. Compressed Sensing (CS) Method

Compressed sensing has been shown to be able to estimate sparse or compressible signals from incomplete measurements [6, 7]. Consider a signal x in R^N. x is sparse if most elements of x are zero. Similarly, x is compressible if most elements of x are near zero. Specifically, x is S-sparse if $\|x\|_0 \le S$, where S is a positive integer and $\|\cdot\|_p$ is the ℓ_p-norm operator defined as

$$\|x\|_p := \left(\sum_{i=1}^{n} |x_i|^p\right)^{1/p}, \quad (10)$$

where p is non-negative integers. Let us further define the set of S-sparse vectors:

$$\Sigma_S := \{x \in R^N : \|x\|_0 \le S\}, \quad \forall S \in \{1, \ \ldots, \ N\}. \quad (11)$$

Then, a vector x' in R^N can be approximated by a vector x in Σ_S, and the approximation error of x' in ℓ_p-norm, $\sigma_S(x')_p$, is

$$\sigma_S(x')_p = \inf_{\mathbf{x}\in\Sigma_S} \|x' - x\|_p, \quad (12)$$

where inf(·) is the infimum operator. If $\sigma_S(x')_p$ is small enough for S, then x' is S-compressible. Regarding the sampling scheme of CS, unlike the uniform sampling of the Nyquist/Shannon theory, CS employs a linear measurement model, that is,

$$y = \Phi x, \quad (13)$$

where y in R^M is the measurement vector, and Φ in $R^{M\times N}$ is the measurement matrix. The interest of CS is that $M << N$, which is considered an underdetermined linear system implying that there are infinite solutions, but keep in mind that x is sparse. By taking advantage of the sparsity of x, one can utilize ℓ_1-minimization to find some optimal solutions of the underdetermined system. The ℓ_1-minimization is defined as

$$\min_x \|x\|_1 \quad \text{subject to} \quad y = \Phi x \cdot \quad (14)$$

In reality, noise is always present, so the following equivalent minimization is more practical:

$$\min_x \frac{1}{2}\|y - \Phi x\|_2^2 + \tau\|x\|_1, \quad (15)$$

where τ is a nonnegative parameter. Note that here the Gradient Projection for Sparse Reconstruction (GPSR) algorithm is employed to solve for x in (15). In general, GPSR is an iterative gradient projection algorithm and was developed by Figueiredo *et al.* [10]. Depending on the line search method, there are two versions of GPSR: 1) GPSR-Basic employing the quasi-Newton line search method, and 2) GPSR-BB employing the Barzilai-Borwein line search method. In this study, we adopted GPSR-BB since it may achieve a faster rate of convergence.

C. CS-based HRV Spectral Estimation

From (9) and (13), it is obvious that if we let $\Phi = A$, then the IPFM-based spectral model can be simply fit by the linear measurement model of CS. The only concern is whether the frequency components a_k and b_k can be represented as a sparse or a compressible signal. We believe that a_k and b_k can be represented as a compressible signal since major characteristics of a standard HRV spectrum are determined by the amplitudes of three main lobes only (two are located at the frequency < 0.15 Hz; while one is at that > 0.15 Hz), and the side lobes can be ignored. So, for the IPFM-based HRV spectral estimation we may take the advantage of using the CS framework to deal with the underdetermined cases. The novel method is able to combat the loss or incorrectness of RR intervals. Our results presented in the subsequent section further demonstrated the robustness of the proposed method.

III. Results and Discussion

To show the ability of GPSR-BB in estimating the IPFM based HRV spectra under the CS framework, first we let $K=(L-1)/2$ such that data loss rate $R = 0$ (*i.e.*, a complete RR set is used) and A is a squared matrix, where R is defined as

$$R = \frac{\#\text{ of lost data}}{\#\text{ of total data}}. \quad (16)$$

Then, we tested this setting on a number of simulated RR intervals generated by the IPFM model and on practical RR intervals derived from a healthy subject to see if the HRV spectra reflect the characteristics as we expected.

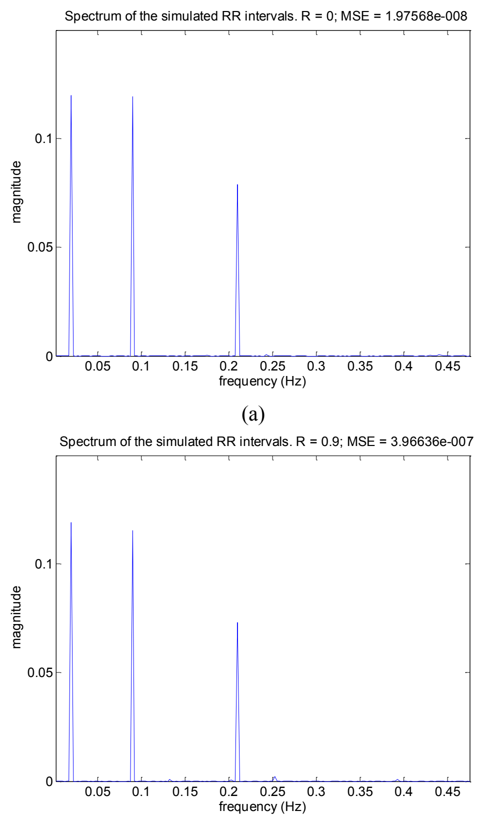

(a)

(b)

Figure 1. (a) The HRV spectrum derived from the complete simulated RR intervals. The MSE between the estimated spectrum and the true spectrum is 1.97568e-008. (b) The HRV spectrum derived from the simulated RR intervals truncated randomly with R = 0.9. The MSE between the estimated spectrum and the true spectrum is 3.96636e-007.

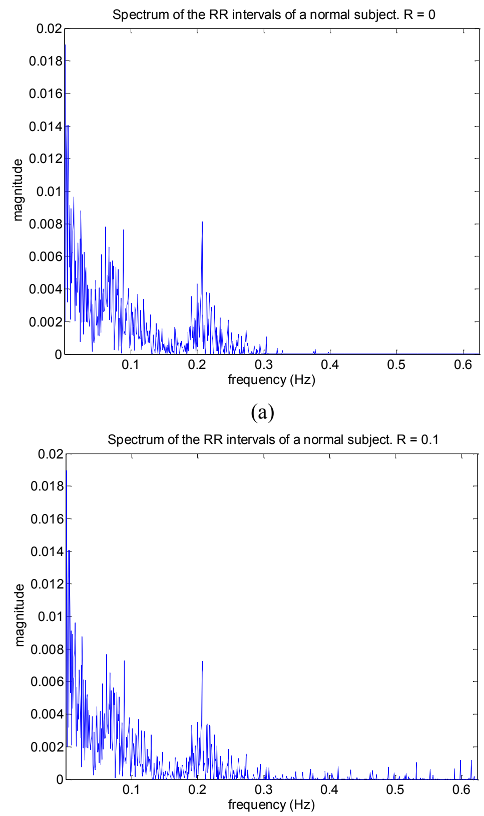

(a)

(b)

Figure 2. (a) The HRV spectrum of a normal subject derived from the complete RR dataset. (b) The HRV spectrum of the normal subject derived from the incomplete RR dataset with R = 0.1 (a randomly-truncated case).

We first generated a set of simulated RR intervals using exactly the same settings in [4], briefly summarized below:

1) TR = 1.05 s

2) $m(t) = m_1\cos(2\pi f_1 t) + m_2\cos(2\pi f_2 t) + m_3\cos(2\pi f_3 t)$ with m_1 = 0.12, m_2 = 0.12, m_3 = 0.08, f_1 = 0.02 Hz, f_2 = 0.09 Hz and f_3 = 0.21 Hz.

3) L = 381

4) T = 400 s

Fig. 1(a) shows the HRV spectrum derived from the complete set of simulated RR intervals by the proposed method. One may see that there are significant frequency components at 0.02 Hz, 0.09 Hz and 0.21 Hz with magnitude almost equal to 0.12, 0.12 and 0.08, respectively. Although there are tiny components at other frequencies, the magnitudes are small enough (usually on the order of 10^{-6} or less) to be ignored. The mean squared error (MSE) between the estimated spectrum and the true spectrum is 1.97568e-008. Next, to further demonstrate the power of CS in estimating HRV spectra from the incomplete set of RR intervals, we shortened the simulated RR time series by removing the RR intervals randomly with R = 0.9 and then compared the spectra derived from incomplete RR intervals with those derived from the complete RR interval dataset previously. As a result, the HRV spectrum estimated from the incomplete RR intervals is as depicted in Fig. 1(b). In fact, Figs. 1(a) and (b) are visually identical, even the latter is obtained from only 10% of the simulated RR intervals (*i.e.*, R = 0.9). The MSE between the spectrum derived from the incomplete simulated RR intervals and the true spectrum is 3.96636e-007, which is still considerably small.

In addition, in our study we also used the RR intervals practically measured from a healthy normal subject to demonstrate the proposed method. The HRV spectrum derived from the complete set of RR intervals is as shown in Fig. 2(a). It is obvious that Fig. 2(a) reveals the characteristics of the standard HRV spectrum of a normal subject, *i.e.*, there are major components seen in a Lower Frequency (LF) band [0.04, 0.15] Hz and a Higher Frequency (HF) band [0.15, 0.40] Hz, which correspond to the sympathetic and vagal activities, respectively. Hence, from Fig. 2(a), the proposed method is shown to be able to achieve HRV spectral estimates from real RR interval data. Similarly, we also estimated the HRV spectrum using the incomplete RR dataset simply by removing 10% of the real RR intervals (*i.e.*, R = 0.1) in a random order. Consequently, the corresponding estimated HRV spectrum is as shown in Fig. 2(b). Observing the figure, we may find that although there are small distortions seen in the higher frequency bands, the locations and the magnitudes of the main lobes in LF and HF bands are almost the same as those of the actual spectrum as depicted in Fig. 2(a). One may notice that while the simulated RR data can tolerate 90% data loss, the real RR data only tolerate 10% data loss. This is because the simulated RR intervals are completely sparse with S = 3 (recall the definition of S in section II-B), whereas the real RR interval data are considered as a compressible signal.

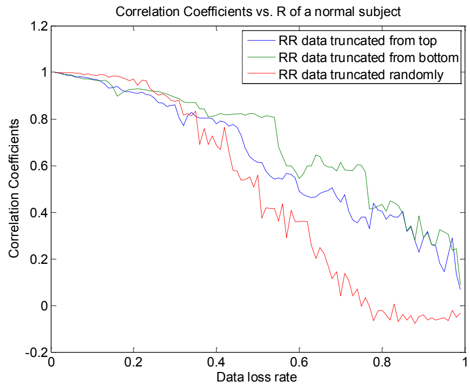

(a)

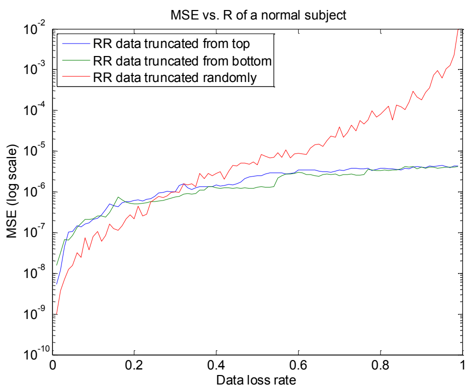

(b)

Figure 3. (a) Correlation coefficients versus R of a normal subject. (b) Mean squared error versus R of a normal subject.

To further investigate the robustness of proposed method in depth, using the RR dataset of the same normal subject we first estimated the true HRV spectrum from the complete RR dataset (as given in the form of a column vector), and then estimated the HRV spectra from incomplete RR datasets formed by truncating the RR intervals in the top, in the bottom, and in a randomly non-consecutive order from the original RR vector with R ranging from 0.01 to 0.99, respectively. We then measured the similarities between the true HRV spectrum and those derived from incomplete RR datasets, respectively, by calculating the Correlation Coefficients (CC) and Mean Squared Error (MSE) among them.

Figs. 3(a) and (b) present the plots of CC versus R and MSE versus R of the normal subject, respectively. It is revealed from these plots that the performances of spectral estimation are almost the same no matter the RR intervals are truncated from the top or from the bottom. Also, the numerical results indicated that the proposed method may tolerate up to 13% and to 14% of data loss caused by truncating the RR intervals from the top and from the bottom, respectively, while CC remains above 0.95 in both cases. On the other hand, although the performance obtained from the incomplete RR dataset formed by randomly truncating the RR intervals appears to degrade faster when R becomes larger, the scenario of randomly truncated case actually makes more sense in practice. As a result, with CC equal to 0.95, the proposed method can tolerate 23% loss of RR data in the randomly truncated case, which is competitive with the performances obtained from the top- and the bottom-truncated cases.

From the results one may see that even though the top- or bottom-truncated RR time series may lose a significant portion of data, the incomplete RR recording formed by the remaining consecutive RR intervals can still well preserve the major spectral characteristics of HRV. On the other hand, since the HRV spectral estimation performance obtained from the randomly truncated RR dataset would quickly degrade when the data loss rate R became large, we may speculate that in the randomly-truncated case more RR data may be required to preserve the major HRV spectral characteristics. However, when R is restricted to an adequately small value (typically below 0.15), the HRV spectral estimation performance on the randomly-truncated case is actually comparable to those on both the top- and bottom-truncated cases.

IV. Conclusion

In general, the IPFM model has been widely accepted as a functional description of the mechanism by which the autonomic nervous system modulates the HR. In this study, a novel HRV spectral estimation method developed by combining the use of the IPFM model and the CS framework is proposed. Tests conducted using the simulated and real RR datasets indicated that the proposed method is capable of providing accurate HRV spectral estimates with a degree of robustness, even when the RR data is incomplete or corrupted due to ectopic or missing beats occurred in practice.

References

[1] S.-W. Chen, "A wavelet-based heart rate variability analysis for the study of nonsustained ventricular tachycardia," *IEEE Trans. Biomed. Eng.*, vol. 49, no. 7, pp. 736–742, 2002.

[2] R. D. Berger, S. Akselrod, D. Gordon and R. J. Cohen, "An efficient algorithm for spectral analysis of heart rate variability," *IEEE Trans. Biomed. Eng.*, vol. 33, no. 9, pp. 900–904, 1986.

[3] O. Rompelman, A. J. R. M. Coenen and R. I. Kitney, "Measurement of heart-rate variability: part 1-comparative study of heart-rate variability analysis methods," *Medical & Biological Engineering & Computing,* vol. 15, no. 3, pp. 233-239, 1977.

[4] I. P. Mitov, "Spectral analysis of heart rate variability using the integral pulse frequency modulation model," *Medical & Biological Engineering & Computing,* vol. 39, no. 3, pp. 348-354, 2001.

[5] F. Chen and Y. T. Zhang, "An efficient algorithm to reconstruct heart rate signal based on an IPFM model for the spectral analysis of HRV," in *Engineering in Medicine and Biology Society, 2005. IEEE-EMBS 2005. 27th Annual International Conference of the*, Shanghai, 2005.

[6] E. J. Candes and M. B. Wakin, "An introduction to compressive sampling," *Signal Processing Magazine, IEEE,* vol. 25, no. 2, pp. 21-30, 2008.

[7] R. G. Baraniuk, E. Candes, R. Nowak and M. Vetterli, "Compressive sampling," *Signal Processing Magazine, IEEE,* vol. 25, no. 2, pp. 12-13, 2008.

[8] K. Choi, J. Wang, L. Zhu, T. S. Suh, S. Boyd and L. Xing, "Compressed sensing based cone-beam computed tomography reconstruction with a first-order method," *Medical Physics,* vol. 37, no. 9, pp. 5113-5125, 2010.

[9] M. Lustig, D. L. Donoho, J. M. Santos and J. M. Pauly, "Compressed sensing MRI," *Signal Processing Magazine, IEEE,* vol. 25, no. 2, pp. 72-82, 2008.

[10] M. A. T. Figueiredo, R. D. Nowak and S. J. Wright, "Gradient projection for sparse reconstruction: application to compressed sensing and other inverse problems," *Selected Topics in Signal Processing, IEEE Journal of,* vol. 1, no. 4, pp. 586-597, 2007.